Superlattices and Microstructures 65 (2014) 195–205

Contents lists available at ScienceDirect

Superlattices and Microstructures

journal homepage: www.elsevier.com/locate/superlattices

Review

Half-metallic ferromagnetism in $Al_{1-x}Cr_xP$ and superlattices $(AlP)_n/(CrP)_m$ by density functional calculations

M. Merabet [a], D. Rached [a,*], S. Benalia [a], A.H. Reshak [b,c], N. Bettahar [a], H. Righi [a], H. Baltache [d], F. Soyalp [e], M. Labair [a]

[a] Laboratoire des Matériaux Magnétiques, Faculté des Sciences, Université Djillali Liabès de Sidi Bel-Abbès, Sidi Bel-Abbès 22000, Algeria
[b] Institute of Complex Systems, FFPW, CENAKVA, University of South Bohemia in CB, Nove Hrady 37333, Czech Republic
[c] Center of Excellence Geopolymer and Green Technology, School of Material Engineering, University Malaysia Perlis, 01007 Kangar, Perlis, Malaysia
[d] Laboratoire de Physique Quantique et de Modélisation Mathématique de la Matière (LPQ3M), Université de Mascara, Mascara 29000, Algeria
[e] Yüzüncü Yıl Üniversitesi, Eğitim Fakültesi, OFMAE Bölümü Fizik Öğretmenliği Anabilimdalı, 65080 Kampüs Van, Turkiye

ARTICLE INFO

Article history:
Received 10 September 2013
Received in revised form 30 September 2013
Accepted 23 October 2013
Available online 29 October 2013

Keywords:
DMSs
Superlattices
Electronic structure
Magnetic properties

ABSTRACT

Using the first-principles full-potential linear muffin-tin orbital (FP-LMTO) method based on density functional theory, we have investigated the electronic structure and magnetism of order dilute ferromagnetic semiconductor $Al_{1-x}Cr_xP$ ($x = 0.125$, 0.25 and 0.50) and the superlattices $(AlP)_1/(CrP)_1$ and $(AlP)_3/(CrP)_1$. For the exchange-correlation functional, the generalized gradient approximation (GGA) has been used. It is shown that these compounds are half-metallic ferromagnets. Calculations of the s-d exchange constant $N_0\alpha$ and p-d exchange constant $N_0\beta$ clearly indicate the magnetic nature of these compounds. We observe that p-d hybridization reduces the local magnetic moment of Cr from its free space charge value and produces small local magnetic moments on the non-magnetic Al and P sites.

* Corresponding author. Tel.: +213 554192664.
E-mail address: rachdj@yahoo.fr (D. Rached).

0749-6036/$ - see front matter © 2013 Elsevier Ltd. All rights reserved.
http://dx.doi.org/10.1016/j.spmi.2013.10.037

Contents

1. Introduction

Semiconductors and magnetic materials both play essential roles in modern electronics industry. Most electronic and optical semiconductor devices utilize the charge of electrons and holes to process information, and magnetic materials use the spin of magnetic ions for information storage. Thus, although the applications of semiconductors and magnetics have evolved independently, it appears logical to combine their properties for possible spin-electronic applications with increased functionalities [1,2]. Historically, coexistence of magnetism and semiconducting properties in diluted magnetic semiconductors (DMSs) has in fact already as early as the 1970s [3]. The dilute magnetic semiconductors are semiconducting alloys whose lattice is made up in part of substitutional magnetic atoms (such as Mn, Cr or Fe). This group of materials has been studied thoroughly for many years because of their unique magneto-transport and magnetooptical properties [4,5]. In those early years, the study of DMSs and their heterostructures was primarily focused on II–VI-based materials (such as those based on HgTe, CdTe, and ZnSe), where the valence of group-II cations is identical to that of many magnetic ions, such as Mn or Co [3]. The transition metal doped III–V semiconductors are widely used in high speed electronic, optoelectronic and spintronics devices [6,7]. Many experiments have been performed successfully in order to search DMS materials of ferromagnetic behavior at room temperature by doping transition metal elements in wide band gap semiconductor such as Mn-doped in InAs, GaAs, while using a variety of experimental techniques Cr-doped AlN thin films have been synthesized and are found to exhibit ferromagnetic properties at room temperature [6–13].

Cr-doped III-V compound is among the DMSs III-V, characterized by its ferromagnetic behavior. This is confirmed by Lin et al. [14]; High quality Cr-doped AlN and GaN thin films have been synthesized on 6H-SiC using reactive MBE. Optimized Al(Cr)N and Ga(Cr)N films were found to be ferromagnetic with Curie temperatures above 900 K. From the theoretical point of view, Katayama and collaborators [15] have investigated in detail by ab initio electronic-structure calculations based on the LSDA using the Korringa–Kohn–Rostoker method combined with the coherent potential approximation (KKR-CPA) the electronic structure of III–V compound-based DMSs. In 2006, Wang and coworkers [16] reports the results of a theoretical study within the framework of density functional theory of magnetic coupling between Cr atoms doped in bulk AlN as well as AlN $(11\bar{2}0)$ thin films having wurtzite structure. Two years later, Zhang and collaborators [17] have studied the electronic and magnetic properties of Cr-doped AlP by using the FPLAPW method implemented in the WIEN2k package. These studies predict Cr-doped AlP to be a robust half-metallic dilute magnetic semiconductor. Very recently, Saeed et al. [18], with using full potential density functional method have been studies the electronic, magnetic and structural properties in zinc blende phase of Cr-doped $Al_{1-x}Cr_xX$ (X = N, P, As, Sb) ternary compounds with $(0 < x \leqslant 0.50)$ concentration has been undertaken.

In this paper, we investigate the structural, electronic and magnetic properties of DMSs $Al_{1-x}Cr_xP$ $(0 < x \leqslant 0.50)$ and the two superlattices $(AlP)_1/(CrP)_1$ and $(AlP)_3/(CrP)_1$ in the zinc-blende structure (B3), by using the full-potential linear muffin-tin orbital (FP-LMTO) method, in the framework of

the density functional theory (DFT) within the generalized gradient approximation (GGA) for the exchange correlation functional by considering the effect of polarized spin. The organization of the article is as follows. The computational method we have adopted for the calculations is described in Section 2. We present our results in Section 3. Finally, conclusions are given in Section 4.

2. Calculation methodology

The rapid increasing in power and speed of computers has been accompanied by considerable advances in techniques that are used to model the electronic structure. These models typically provide accurate predictions of the ground state energy and internal forces in many systems. In this work, the FP-LMTO method as implemented in the Lmtart computer code [19,20], has been applied to perform first-principles total energy calculations. This method is based on the DFT which is a universal quantum mechanical approach for many body problems. In this approach the quantum many body problem of an interacting electron gas is mapped exactly onto a set of single particles moving in an effective local potential with same density as is real, and the obtained one electron equations are called Kohn–Sham equations [21,22]. The space in this method is divided into an interstitial region (IR) and non-overlapping muffin-tin (MT) spheres centered at the atomic sites. In the IR region, the basis functions are represented by Fourier series. Inside the MT spheres, the basis functions are expanded in combinations of spherical harmonics functions. A description of this method can be found in Ref. [20]. The exchange and correlation effects were treated by the generalized gradient approximation of Perdew et al. (GGA) [23]. Details of calculations are as follows: the charge density and the potential are represented inside the muffin-tin spheres (MTS) spherical harmonics up to $l_{max} = 6$. The k integration over the Brillouin zone is performed using the tetrahedron method [24]. The values of the sphere radii (MTS) and the number of plane waves (NPLW) used in our calculation are listed in Table 1.

3. Results and discussions

3.1. Structural properties

In this subsection, we calculate the structural properties in the cubic phase of the compounds AlP, CrP, their alloys for different concentrations x and their superlattices composed of different layers of these compounds. For the ternary alloy we have chosen the basic cubic cell as unit cell so that the alloys have been modeled at some selected compositions $x = 0.125$, 0.25, and 0.5. For the concentration $x = 0.125$, we considered $1 \times 1 \times 2$ supercell with 16 atoms, we followed the same procedure as that of Saeed et al. [18]. The composition $x = 0.25$, we considered the unit cell with four *P* anions and three *Al* and one *Cr*, and finally for $x = 0.5$, we considered two *Al* and two Cr. For superlattices, the description of their structures is as follows: The $(AlP)_1/(CrP)_1$ superlattice consists of alternating one layer of magnetic CrP (the $x = 1$ end member of the $Al_{1-x}Cr_xP$ series) and one layer of nonmagnetic AlP (the $x = 0$ end-member) and the $(AlP)_3/(CrP)_1$ superlattice consists of alternating one layer of magnetic CrP

Table 1
Parameters used in the calculations: number of plane wave (NPW), energy cutoff (in Rydbergs) and the muffin-tin radius (RMT in atomic units).

Compounds	NPLW (Total)	E_{cut} (Ryd)	MTS (a.u)		
			Al	P	Cr
AlP	5064	107.1711	2.185	2.274	–
CrP	5064	120.8395		2.142	2.058
$Al_{0.875}Cr_{0.125}P$	66,800	150.3045	2.263	2.174	2.174
$Al_{0.75}Cr_{0.25}P$	33,400	152.3787	2.248	2.159	2.159
$Al_{0.5}Cr_{0.5}P$	33,400	158.2300	2.206	2.119	2.119
$(AlP)_1/(CrP)_1$	16,242	155.6911	2.115	2.201	2.115
$(AlP)_3/(CrP)_1$	32,458	151.5589	2.180	2.193	2.166

and three layer of nonmagnetic AlP. In our case we chose the [0 0 1] axis as the axis of growth (x and y axes parallel to the layer and z axis perpendicular to it).

In order to determine the equilibrium geometry for the studied compounds, a set of different volumes around the experimental value are chosen and for each volume the total energies are computed. The obtained total energies versus volumes of Cr-doped AlP, $(AlP)_1/(CrP)_1$ and $(AlP)_3/(CrP)_1$ compounds are fitted by Birch's equation of state [25] to determine the ground state properties such as the equilibrium lattice parameters a, the bulk modulus B and its pressure derivative B'. The quantities a, B and B', for different concentrations of Cr (0, 0.125, 0.25, 0.50, 1) in AlP and the superlattices $(AlP)_1/(CrP)_1$ and $(AlP)_3/(CrP)_1$ are redisplayed in Table 2, which also contains experimental and theoretical data for comparison. The calculated equilibrium lattice constant value for AlP compound agree well with the available theoretical results [26,30]. In comparison with the experimental data we find that the lattice constant parameter is underestimated. By contrast, we remark that the lattice constant of CrP compound is underestimated with available theoretical results [36,37]. However, for the alloys our results are in good agreement with theoretical results [18]. The calculated values of the bulk modulus decrease from CrP to AlP, i.e. from the lower to the higher atomic number. This suggests that CrP is more compressive than AlP. The calculated equilibrium parameters (a_0, B_0 and B'_0) in two superlattices are also given in Table 2 we found that $a_{1,3}$ is about twice $a_{1,1}$. To the best of our knowledge, the equilibrium parameters of the superlattices have not yet been measured or calculated. Hence our results can be considered as a prediction study. We find also that the bulk modulus increases with the concentration x in structure of (Al, Cr) P and with the number of monolayer's in structure of superlattices.

3.2. Electronic and magnetic properties

The spin-polarized band structures of ferromagnetic compounds AlCrP ($x = 0.125$, 0.25 and 0.50) and the superlattices $(AlP)_n/(CrP)_m$ ($n = m = 1$, $n = 3$ and $m = 1$) are calculated at the equilibrium lattice constants. Figs. 1–3 show the band spin-polarized band structures of AlCrP ($x = 0.125$) and the superlattices SL_{1-1} and SL_{3-1}, respectively. These figures show for each concentration and layer, the band

Table 2
The calculated equilibrium constant a (Å), bulk modulus B (GPa) and B' (GPa) for $Al_{1-x}Cr_xP$ and superlattices $(CrP)_1/(AlP)_1$ and $(CrP)_1/(AlP)_3$.

Compounds	a (Å)	B (GPa)	B' (GPa)
AlP	**5.45**; 5.451[a];5.4672[e]; 5.436[b];5.511[b]; 5.520[c] 5.535[d]; 5.40[g] 5.434[i]	**86.86**; 86[a]; 86.00[f]; 82[b]; 89[b]; 96[c]; 01[d]; 89.1[h]; 89.1[i]	**4.144**; 3.99[b,h], 4.14[b], 3.90[i]
$Al_{0.875}Cr_{0.125}P$	**5.42** 5.419[i]	**87.90** 88.62[i]	**4.05** 4.10[i]
$Al_{0.75}Cr_{0.25}P$	**5.38** 5.404[i]	**88.7827** 89.40[i]	**3.965** 4.25[i]
$Al_{0.5}Cr_{0.5}P$	**5.28** 5.364[i]	**98.1902** 89.80[i]	**4.0497** 3.55[i]
CrP	**5.12** 5.48[j], 5.35[k], 5.39[l], 5.48[m], 5.42[m], 5.35[m]	**123.6197**	**3.82887**
$(AlP)_1/(CrP)_1$	**5.27**	**101.8650**	**3.98596**
$(AlP)_3/(CrP)_1$	**10.69**	**118.1810**	**2.6829**

[a] Ref. [26].
[b] Ref. [27].
[c] Ref. [28].
[d] Ref. [29].
[e] Ref. [30].
[f] Ref. [31].
[g] Ref. [32].
[h] Ref. [33].
[i] Ref. [18].
[j] Ref. [34].
[k] Ref. [35].
[l] Ref. [36].
[m] Ref. [37].

structures corresponding to spin up and spin down alignments we found that the compounds are half-metallic. Note that in these half- metallic the majority-spin channel is metallic, while there is a semi-conducting gap in the minority-spin channel. The figures show that of this compound at concentration $x = 0.125$ has a direct band gap Γ–Γ but with increasing concentration, the compound take the same behavior as CrP i.e. an indirect gap Γ–Δ. The point of high symmetry Δ is between Γ-M and Γ-R for the concentrations to 0.25 and 0.50, respectively. For the superlattices, the compound has a indirect gap Γ–Δ and Γ–Δ for SL_{1-1} and SL_{3-1}, respectively. The point of high symmetry Δ is between R-X. The calculated energy band gap values for minority-spin are listed in Table 3, the half-metallic gap (G_{HF}) is determined as the minimum between the lowest energy of majority (minority)-spin conduction bands with respect to the Fermi level and the absolute values of the highest energy of the majority (minority)-spin valence bands. We note that our results are close for the alloys at $x = 0.125$ and 0.25 with those of Saeed et al. [18], a reverse situation was found for the alloy at $x = 0.5$, our band-gap is higher, which is probably due to fact that they used the LDA approximation.

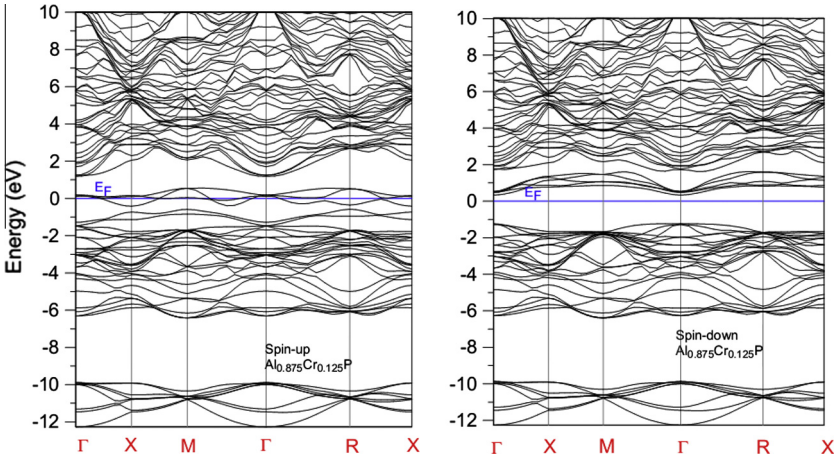

Fig. 1. Spin-dependent band structures of $Al_{0.875}Cr_{O.125}P$.

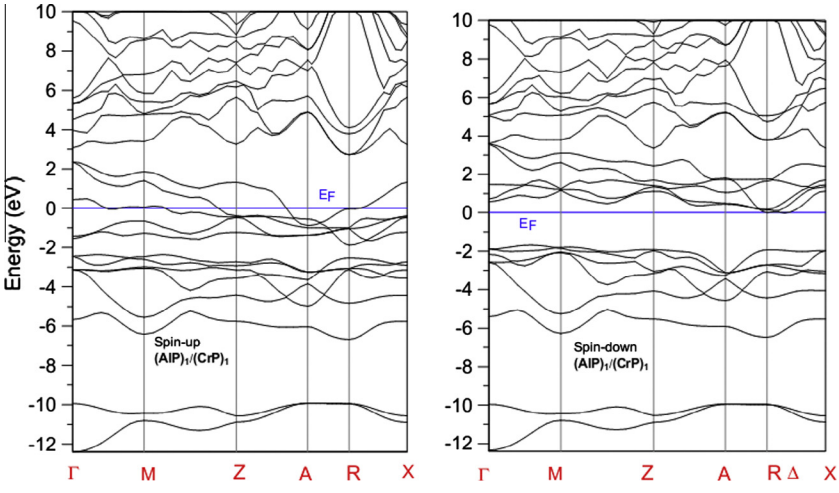

Fig. 2. Spin-dependent band structures of $(AlP)_1/(CrP)_1$.

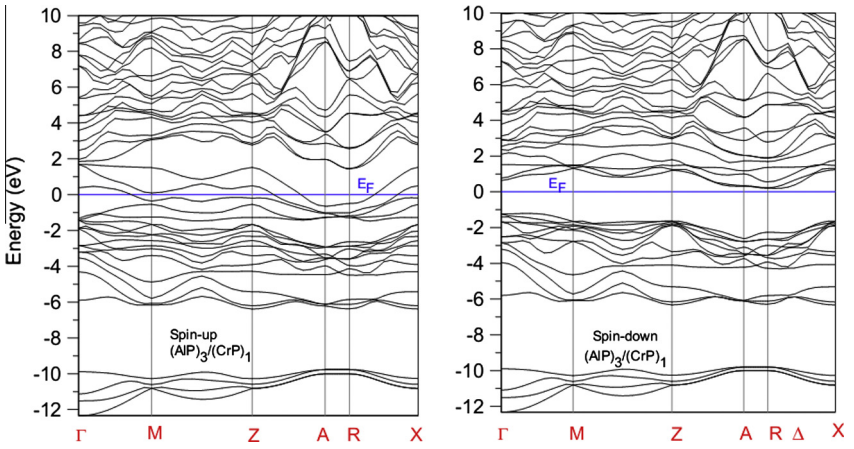

Fig. 3. Spin-dependent band structures of $(AlP)_3/(CrP)_1$.

In order to understand the effect of contribution of Cr at various concentrations and layers about the alloys and superlattices; we determined the spin density of states (DOS). Figs. 3–5 show the calculated spin resolved total and partial densities of states of alloys and superlattices at their equilibrium lattice constants. We found that these figures confirm the half-metallicity of these compounds. We see that the lowest bands in majority spin are mainly formed by the P-3s states with slight contribution of Al-3s and 3p states. The states between ∼−6.4 and −5 eV originate from Al-3s states with few contributions P-3p an Al-3p states. The structure from −5 eV to Fermi level is essentially dominated by *Cr*-3d and P-3p states. The Cr-3d sates are split into a doublet e_g symmetry and triplet with t_{2g} symmetry, respectively. We remark that *Cr*-t_{2g} states are mainly ∼−3 and −2 eV by contrast the *Cr*-e_g states are mainly between ∼−1.5 and −0.8 eV. After the last value *Cr*-t_{2g} states are partially filled which lie midst of the Fermi level, cause the metallic nature of the ternary alloys and superlattices [18]. The total DOS vicinity of the Fermi level (E_F) shows a gap for the different concentrations and layers for minority-spin which a good agreement with the previous theoretical values [18]. The same contributions for minority-spin for the lowest bands expected between ∼−1.9 and −1 eV the Cr-t_{2g} are more dominant (see Fig. 6).

It is instructive to understand the mechanism ferromagnetism in these compounds (alloys and superlattices). The states t_{2g} are lower in energy than e_g states. Since, the magnetic moment of these compounds originate mainly from t_{2g} states of the *Cr* atom. The t_{2g} states are strongly spin split and are situated close the Fermi level, resulting in the partial occupation of the spin-up states. We remark also

Table 3
Calculated energy gap E_g in semiconducting spin channel, half-metallic gap G_{HF}, the exchange spin splitting at the conduction (ΔE_c) and valence (ΔE_v) band edges and the exchange constants $N_0\alpha$ and $N_0\beta$ (units are in eV).

Compounds	E_g	G_{HF}	ΔE_c	ΔE_v	$N_0\alpha$	$N_0\beta$
$Al_{0.875}Cr_{0.125}P$	1.55 1.65[a]	0.33	0.064	−1.234	0.256	−4.936
$Al_{0.75}Cr_{0.25}P$	1.69 1.6[a]	0.19	0.45	−1.56	0.9	−3.12
$Al_{0.50}Cr_{0.50}P$	1.85 1.6[a]	0.63	0.89	−1.291	0.89	−1.291
SL_{1-1}	1.69	0.0	0.173	−1.559	0.346	−3.118
SL_{1-3}	1.43	0.2	–	–	–	–

[a] Ref. [18].

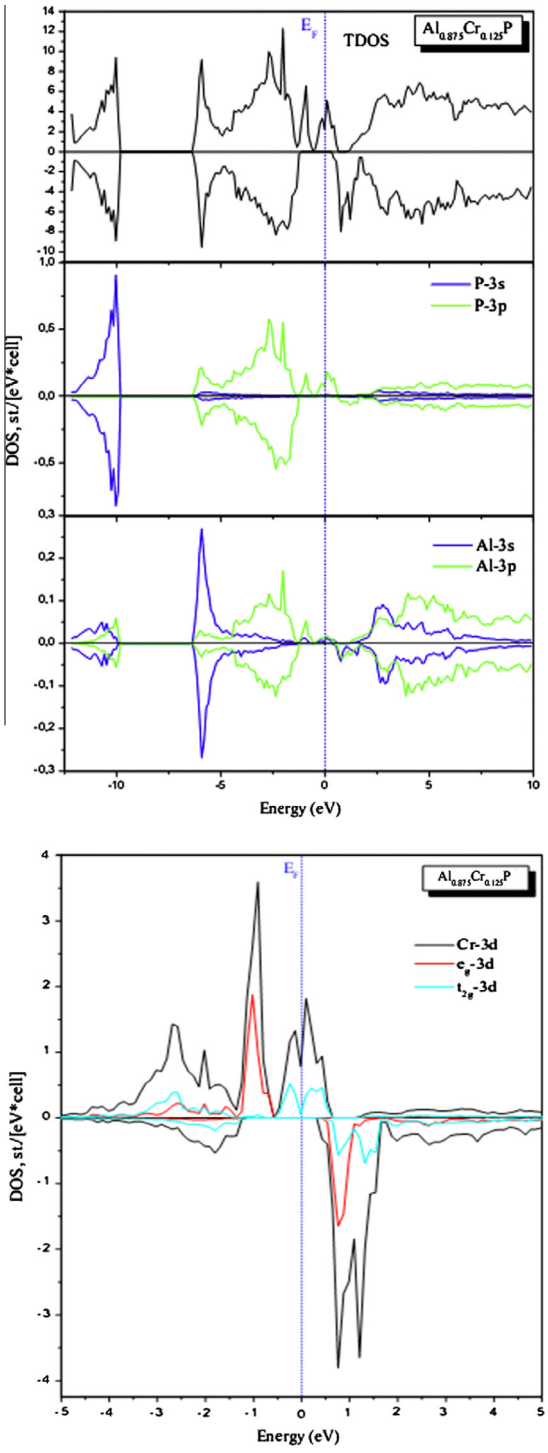

Fig. 4. Spin-dependent Total and partial DOSs of $Al_{0.875}Cr_{O.125}P$.

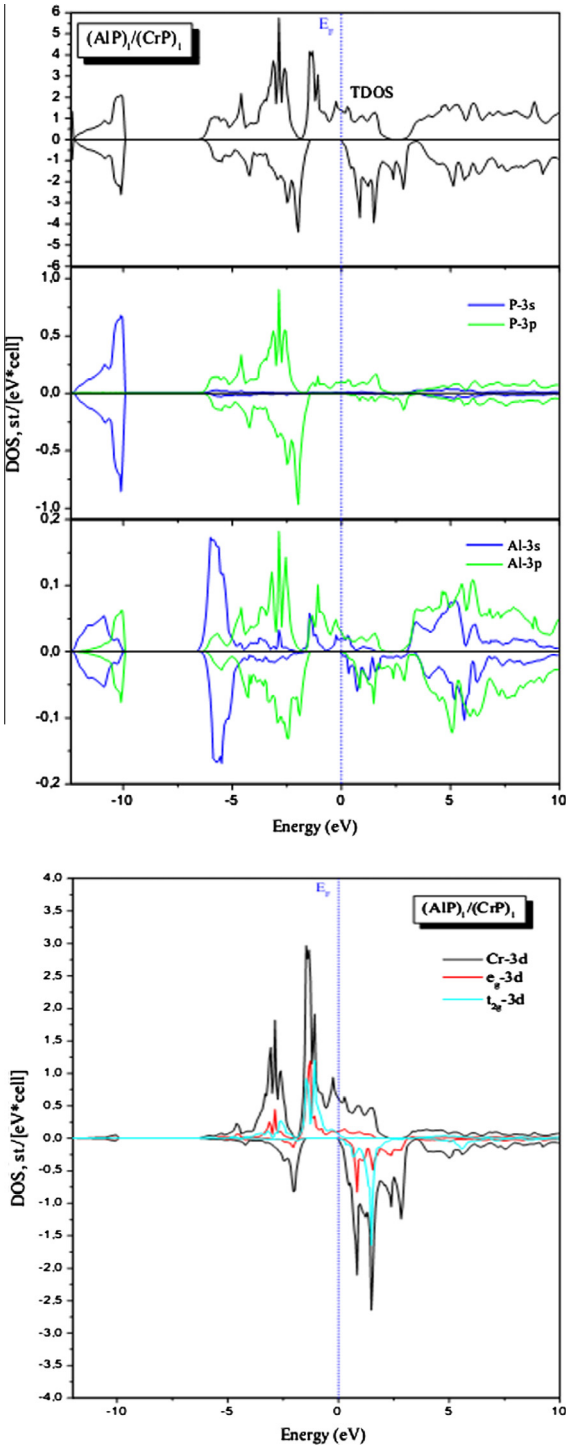

Fig. 5. Spin-dependent Total and partial DOSs of $(AlP)_1/(CrP)_1$.

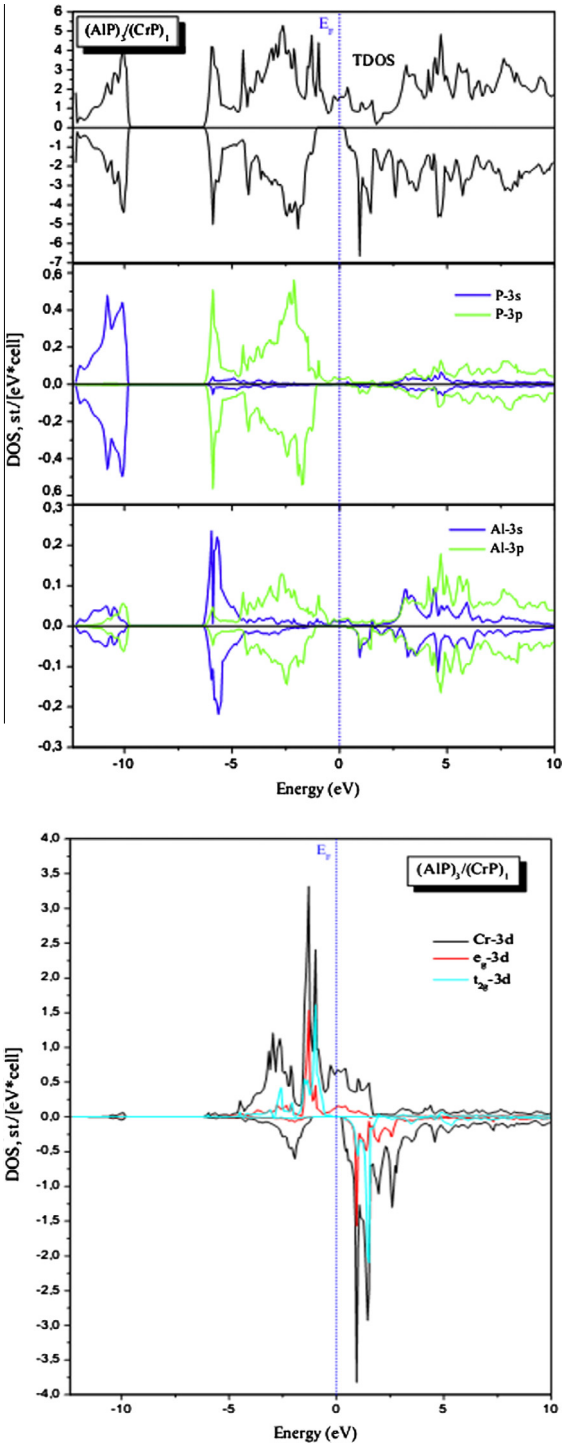

Fig. 6. Spin-dependent Total and partial DOSs of $(AlP)_3/(CrP)_1$.

Table 4
Calculated total magnetic moments, atomic magnetic moments of Cr and interstitial moment (in μ_B) of alloys and superlattices.

Site	$Al_{0.875}Cr_{0.125}P$	$Al_{0.75}Cr_{0.25}P$	$Al_{0.50}Cr_{0.50}P$	SL_{1-1}	SL_{1-3}
M^{tot}	3.0	3.0	6.0	3.0	3.0
	3.0[a]	3.0[a]	3.0[a]	–	–
$m^{interstitial}$	0.477	0.5235	0.5695	0.496	0.460
	0.03885[a]	0.36792[a]	0.3688[a]		
m^{Cr}	2.547	2.875	3.024	2.590	2.662
	2.6766[a]	2.7163[a]	2.7011[a]		

[a] Ref. [18].

the presence of *P*-3p states in the same region of t_{2g} induces the concept of the double exchange (DE) [38]; the P-3p states are coupled with Cr-t_{2g} ones and this leads to ferromagnetic coupling.

The significant parameters defining the magnetic properties of DMSs are the s-d exchange constant $N_0\alpha$ and P-d exchange constant $N_0\beta$ which come from the mean field theory based on the following Hamiltonian [39,40]:

$$H = -N_0\beta s.S$$

where β is the p-d exchange integral, while s and S are the hole spin and *Cr* spin, respectively. The exchange constants are therefore defined directly by:

$$N_0\alpha = \frac{\Delta E_c}{x\langle S\rangle}, \quad N_0\beta = \frac{\Delta E_v}{x\langle S\rangle}$$

$\Delta E_c = E_c\downarrow - E_c\uparrow$ is the s-d exchange spin splitting between the minority and majority spins calculated at the conduction band edge. $\Delta E_v = E_v\downarrow - E_v\uparrow$ is p-d exchange splitting at the valence band maximum edge between the minority and majority spins. The corresponding parameters are calculated and presented in Table 3, except for the SL_{3-1}, wherein the shape of the band structure is not enabled to calculate these values. At first, the trend observed in ΔE_v agrees well with the explanation given above, otherwise, the negative values obtained indicate an AFM alignment arising from p-d exchange splitting, secondly, the positive value of ΔE_c means that the Cr d states are higher in energy than Al states. These results confirm the magnetic nature of these compounds.

Our calculated results for total and local magnetic moments for DMSs $Al_{1-x}Cr_xP$ and superlattices (SL_{1-1} and SL_{3-1}) within muffin-tin spheres as well as in the interstitial sites are listed in Table 4. For comparison, since theoretical data are available for $Al_{1-x}Cr_xP$ [18]. Results show that of Al and P are negligible in comparison to that of Cr and total magnetic moments. From Table 4, the value of the magnetic moments of Cr is between 2.5 and 3.0 depending on the concentration and the monolayers, these values are due to the partially occupied Cr-3d level. The total magnetic of $Al_{0.5}Cr_{0.5}P$ is 6.0 μ_B this is due to two Cr atoms per cell. We note that there is strong hybridization between *3d*-t_{2g} and *P*-p states preserves the total integer moments.

4. Conclusions

In summary, we have used the FP-LMTO method on density functional theory to investigated the electronic structure and ferromagnetism of order DMSs $Al_{1-x}Cr_xP$ ($0 < x \leqslant 0.50$) and the superlattices $(AlP)_1/(CrP)_1$ and $(AlP)_3/(CrP)_1$. These systems are half-metallic, which at $x = 0.125$ the alloy has a direct band gap Γ–Γ but with increasing the concentration, these compounds take the same behavior as CrP. Additionally, values of the exchange constants have been calculated and the total magnetic moments of the DMSs and the superlattices are analyzed. It is also found the p-d hybridization of states Cr-3d(t_{2g}) and P-p states reduces the magnetic moments of Cr ions from its free space change value and produced the local magnetic moments on the non-magnetic Al and P sites.

Acknowledgments

For the authors, this work was supported by Algerian National Project (PNR).

For the author A.H. Reshak his work was supported from the Project CENAKVA (No. CZ.1.05/2.1.00/01.0024). School of Material Engineering, Malaysia University of Perlis, P.O. Box 77, d/a Pejabat Pos Besar, 01007 Kangar, Perlis, Malaysia.

References

[1] G.A. Prinz, Science 250 (1990) 1092.
[2] S.A. Wolf, D.D. Awschalom, R.A. Buhrman, J.M. Daughton, S. von Molnàr, M.L. Roukes, A.Y. Chtchelkanova, D.M. Treger, Science 294 (2001) 1488.
[3] J.K. Furdyna, J. Kossut, Semiconductors and Semimetals, vol. 25, Academic Press, New York, 1988.
[4] J.K. Furdyna, J. Appl. Phys. 64 (1988) R29.
[5] T. Jungwirth, J. Sinova, J. Masek, J. Kucera, A.H. MacDonald, Rev. Mod. Phys. (2006).
[6] A.H. MacDonald, P. Spiffier, N. Samarth, Nat. Mater. 4 (2005) 195.
[7] S.A. Wolf, D.D. Awschalom, R.A. Buhrman, J.M. Daughton, S. von Molnar, M.L. Roukes, A.Y. Chtchelkanova, D.M. Treger, Science 294 (2001) 1488.
[8] I. Zutic, J. Fabian, S.D. Sarma, Rev. Mod. Phys. 76 (2004) 323.
[9] H. Munekata, H. Ohno, S. von Molnar, A. Segmuller, L.L. Chang, L. Esaki, Phys. Rev. Lett. 63 (1989) 1849.
[10] H. Ohno, A. Shen, F. Matsukura, A. Oiwa, A. Endo, S. Katsumoto, Y. Iye, Appl. Phys. Lett. 69 (1996) 363.
[11] D. Kumar, J. Antifakos, M.G. Blamire, Z.H. Barber, Appl. Phys. Lett. 84 (2004) 5004.
[12] S.Y. Wu, H.X. Liu, L. Gu, R.K. Singh, L. Budd, M. van Schilfgaarde, M.R. McCartney, D.J. Smith, N. Newman, Appl. Phys. Lett. 82 (2003) 3047.
[13] S.G. Yang, A.B. Pakhomov, S.T. Hung, C.Y. Wong, Appl. Phys. Lett. 81 (2002) 2418.
[14] Gu Lin, Stephen Y. Wu, H.X. Liu, R.K. Singh, N. Newman, David J. Smith, Magn. Magn. Mater. 290 (2005) 1395.
[15] H. Katayama-Yoshida, K. Sato, Physica B 327 (2003) 337.
[16] Q. Wang, A.K. Kandalam, Q. Sun, P. Jena, Phys. Rev. B 73 (2006) 115411.
[17] Y. Zhang, W. Liu, H. Niu, Solid State Commun. 145 (2008) 590.
[18] Y. Saeed, A. Shaukat, S. Nazir, N. Ikram, Ali H. Reshak, J. Solid State Chem. 183 (2010) 242.
[19] S. Savrasov, D. Savrasov, Phys. Rev. B 46 (1992) 12181.
[20] S.Y. Savrasov, Phys. Rev. B 54 (1996) 6470.
[21] P. Hohenberg, W. Kohn, Phys. Rev. B 136 (1964) 864.
[22] W. Kohn, L.J. Sham, Phys. Rev. A 140 (1965) 1133.
[23] J.P. Perdew, K. Burke, Y. Wang, Phys. Rev. B 54 (1996) 16533.
[24] P. Blochl, O. Jepsen, O.K. Andersen, Phys. Rev. B 49 (1994) 16223.
[25] F. Birch, J. Geophys. Res. 83 (1978) 1257.
[26] R.W.G. Wyckoff, Crystal Structures, second ed., Krieger, Malabar, 1986.
[27] Rashid Ahmed, Fazal-e-Aleem, S. Javad Hashemifar, Hadi Akbarzadeh, Physica B 403 (2008) 1876.
[28] O. Madelung, Landolt-Bornstein, Numerical Data and Functional Relationships in Science and Technology New Series, Springer, Berlin, 1982.
[29] P. Kocinski, M. Zbroszczyk, Semicond. Sci. Technol. 10 (1995) 1452.
[30] I. Vurgaftman, J.R. Meyer, L.R. Ram-Mohan, J. Appl. Phys. 89 (2001) 5815.
[31] M.L. Cohen, Phys. Rev. B 32 (1985) 7988.
[32] P. Rodríguez-Hernández, A. Munoz, Semicond. Sci. Technol. 7 (1992) 1437.
[33] M.J. Herrera-Cabrera, P. Rodríguez-Hernández, A. Munoz, Phys. Stat. Sol. (b) 223 (2001) 411.
[34] R. Gul, C. Sunglae, S.C. Hong, J. Magn. Magn. Mater. 310 (2007) 2192.
[35] R. Gul, Phys. Rev. B 81 (2010) 134410.
[36] K.L. Yao, G.Y. Gao, Z.L. Liu, L. Zhu, Solid State Commun. 133 (2005) 301.
[37] J.E. Pask, L.H. Yang, C.Y. Fong, W.E. Pickett, S. Dag, Phys. Rev. B 67 (2003) 224420.
[38] C. Zener, Phys. Rev. 81 (1951) 440.
[39] S. Sanvito, P. Ordejon, N.A. Hill, Phys. Rev. B 63 (2001) 165206.
[40] B.E. Larson, K.C. Hass, H. Ehrenreich, A.E. Carlsson, Phys. Rev. B 37 (1988) 4137.